

Vectorized coding for Monte Carlo simulation of the one-dimensional quantum spin system

Yutaka Okabe and Macoto Kikuchi

Department of Physics, Tohoku University, Aoba, Sendai, 980, Japan

(Received 26 June 1986)

We implement a high-speed algorithm for Monte Carlo simulation of the quantum spin system using the Suzuki-Trotter formula. The calculation is fully vectorized by decomposing into appropriate sublattices. We introduce a "plaquette" spin representation using logical commands. In order to check the efficiency of our algorithm, we study the one-dimensional *XY* model for the Trotter number $m \leq 32$. Excellent agreement with the exact solution is obtained.

I. INTRODUCTION

Various quantum systems have been studied extensively using the Suzuki-Trotter formula.¹ A d -dimensional quantum system is mapped on to a $(d + 1)$ -dimensional classical system in this formula. The partition function is numerically evaluated by the transfer-matrix method.²⁻⁴ or the Monte Carlo method.⁵⁻⁸ The quantum system is exactly reproduced when the Trotter number m tends to infinity. Large m should be used at low temperatures where quantum effects are important. However, the Trotter numbers employed in previous numerical simulations are not so large, due to the memory size of a computer in the case of the transfer-matrix method, and due to the computation time in the case of the Monte Carlo method.

Recently marked progress has been made in the speed-up of Monte Carlo simulation of classical systems.⁹⁻¹¹ The use of vector computers and the development of an efficient algorithm have made the speedup possible. The speeds of Monte Carlo simulations of the three-dimensional Ising model with periodic boundary conditions are often compared. Using a vector computer NEC SX-2 (SX-1), we have realized the speed of 34×10^6 (17×10^6) spin-flip attempts per second. It is desirable that such a technique of speedup is applied to quantum statistical Monte Carlo simulations.

In this paper we report the vectorized Monte Carlo simulation of a quantum spin system. We use the logical command XOR (exclusive OR) for the speedup of the simulation. The one-dimensional quantum *XY* model is studied for the Trotter number $m = 8, 16,$ and 32 . We carefully examine the large m behavior of the energy and the specific heat.

II. HIGH-SPEED QUANTUM MONTE CARLO SIMULATION

We treat the one-dimensional quantum spin system described by the Hamiltonian

$$\mathcal{H} = -2 \sum_{i=1}^N (J_x s_i^x s_{i+1}^x + J_y s_i^y s_{i+1}^y + J_z s_i^z s_{i+1}^z). \quad (1)$$

According to the Suzuki-Trotter formula¹ we approximate the partition function as

$$Z = \text{Tr} \exp(-\beta \mathcal{H}) \simeq \text{Tr} \left[\prod_j \exp(-\beta \mathcal{H}_j / m) \right]^m, \quad (2)$$

where \mathcal{H}_j are the local interactions such that $\mathcal{H} = \sum_j \mathcal{H}_j$, and m is called the "Trotter number." The present system is mapped onto the two-dimensional $(N \times 2m)$ Ising model with four-spin interactions by the use of checkerboard decomposition.¹² The graphical representation of the checkerboard decomposition is given in Fig. 1, where the shaded squares denote the four-spin interaction. Only eight four-spin configurations are allowed for $S = \frac{1}{2}$, and they are graphically shown in Fig. 2. For the special symmetrical case $J_x = J_y$ the matrix elements of two four-spin configurations become zero. Let us introduce a convenient representation. We regard a four-spin configuration as a single information and call it a "plaquette" spin p . There are $N \times m$ plaquette spins as a total in our system. We assign 0-7 to each state of the plaquette spin. The binary-number representation of the assignment is also given in Fig. 2. In updating the four-spin configuration, we should flip even classical spins in the square because of the conservation law. The spin flip is simply realized by the logical command XOR in our plaquette spin representation. The plaquette spin has three bits, and the command XOR is operated on each bit. Fig.

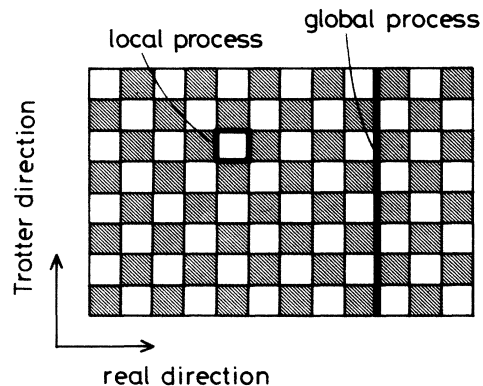


FIG. 1. Graphical representation of the checkerboard decomposition. The shaded squares denote the four-spin interaction. Periodic boundary condition is imposed along the Trotter direction. The local and global spin-flip processes are also illustrated.

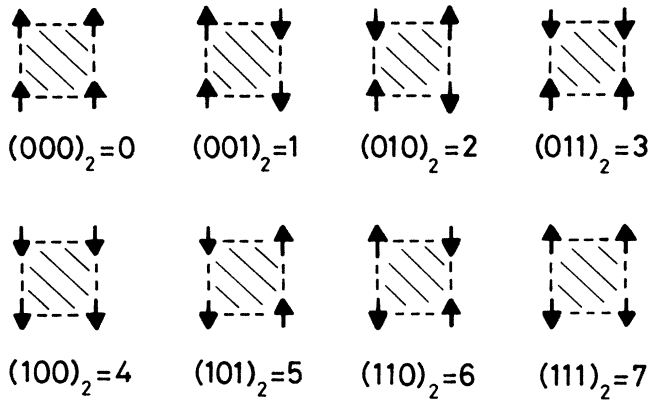


FIG. 2. "Plaquette" spin representation of the four-spin configuration.

ure 3 gives the mathematical expression for pair flips. The encircled spins are flipped. The four-spin flip process is represented by $p_{\text{new}} = \text{XOR}(p_{\text{old}}, 4)$ in the present notation. Since the plaquette spin has the information on the four-spin configuration, we can readily calculate the energy, the specific heat, the magnetization, etc.^{7,12} The energy E and the specific heat C are calculated by the energy of the local Hamiltonian $E_j^{(m)}$ through the relations⁷

$$E = \langle F^{(m)} \rangle, \tag{3}$$

$$CT^2 = \langle (F^{(m)})^2 \rangle - \langle F^{(m)} \rangle^2 - \langle G^{(m)} \rangle, \tag{4}$$

where $F_j^{(m)}$ and $G_j^{(m)}$ are, respectively, defined by

$$F_j^{(m)} = \frac{\partial}{\partial \beta} (\beta E_j^{(m)}), \tag{5}$$

$$G_j^{(m)} = \frac{\partial^2}{\partial \beta^2} (\beta E_j^{(m)}). \tag{6}$$

Since there are some misprints in Ref. 7, we present the expressions for $E_j^{(m)}$, $F_j^{(m)}$, and $G_j^{(m)}$ in the Appendix. We should note that our representation is also useful for the calculation of correlation functions.

Next consider the vectorization of Monte Carlo simulations. Generally, the calculation is fully vectorized⁹⁻¹¹ if the following condition is satisfied: One divides the lat-

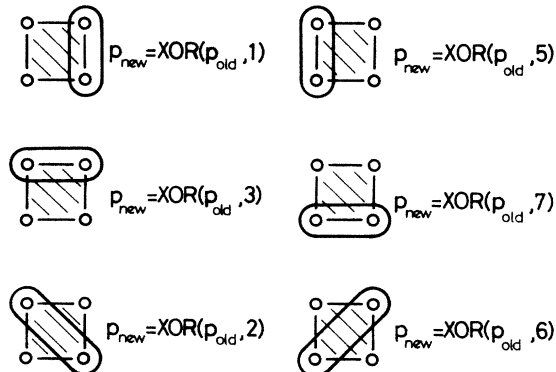


FIG. 3. Mathematical expression for the pair spin flip in the "plaquette" spin representation. The encircled spins are flipped.

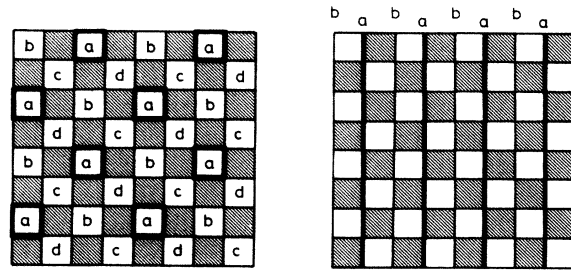


FIG. 4. Subgroup decomposition of the Monte Carlo trials for the local and global processes.

tice into interpenetrating sublattices so that one can update spins on each sublattices independently. Such a decomposition is always possible if the interaction is of short range. In our Monte Carlo simulation of the one-dimensional quantum spin system, we should treat multi-spin-flip processes.¹³ We employ both local and global processes to update the spin configuration.⁸ Both processes are graphically shown in Fig. 1. All the spins on the bold line are flipped according to the transition probability determined by the change of local energy at the spin flip. The local (global) process is important at low (high) temperatures.¹³ We can vectorize the calculation for both processes. For the local process we divide the local-flip loops into four groups. The illustration of the subgroups is given in Fig. 4. In the Monte Carlo trial one only needs the information on neighboring plaquette spins. Then the spin flip on each subgroup is performed in parallel. For the global process, we divide our lattice into two sublattices, and the calculation is fully vectorized. The subgroup for the global process is also shown in Fig. 4.

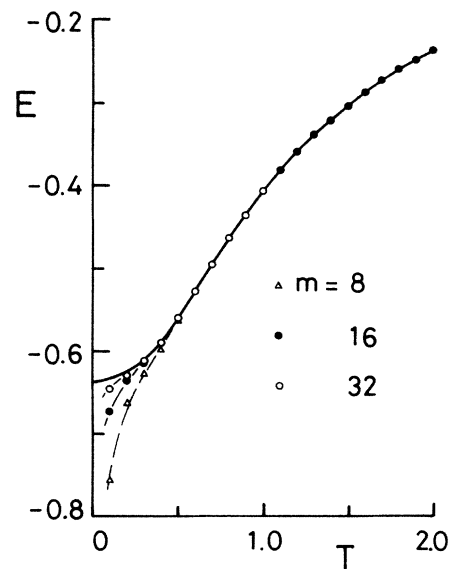


FIG. 5. Temperature dependence of energy for the one-dimensional XY model for $m=8, 16,$ and 32 in units of J . The solid curve is the exact solution of Katsura (Ref. 14).

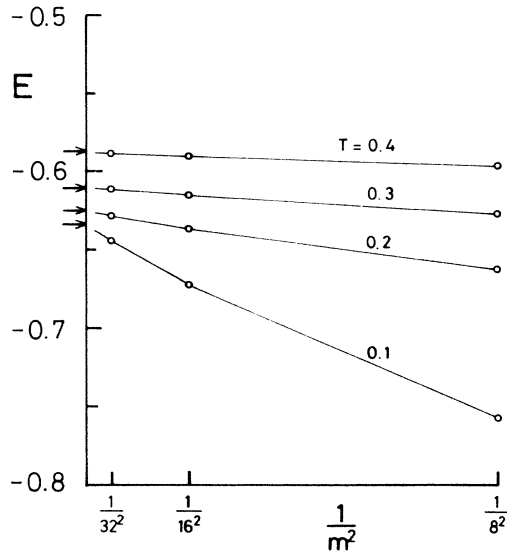


FIG. 6. Energies versus $1/m^2$ for the one-dimensional XY model at fixed temperatures. The arrows indicate the exact values obtained by Katsura (Ref. 14).

One comment should be made here on the ergodicity of the simulation. Exactly speaking, our simulation is not ergodic only by two processes, that is, the local and global processes shown in Fig. 1. The global process to flip all the spins on the horizontal line, for example, should be added for the ergodicity.⁸ This process becomes important for small N and at low temperatures. We have checked for the parameters used in the present study that the contribution from this process is negligibly small.

III. ONE-DIMENSIONAL XY MODEL

We have carried out the Monte Carlo simulation of the one-dimensional XY model by the vector computer NEC SX-1 of the computer center of Tohoku University. We have mainly treated the case $J_x = J_z = J$, $J_y = 0$. We have also dealt with the case $J_x = J_y = J$, $J_z = 0$ to check the consistency. The number of the spins and the Trotter number are $N = 128$, and $m = 8, 16$, and 32 . We define a single Monte Carlo step by updating all the mapped classical spins ($N \times 2m$). The number of Monte Carlo steps is 2×10^5 , 4×10^5 , and 8×10^5 for $m = 8, 16$, and 32 , respectively. We have performed two independent runs for each parameter. The ratio of the local process to the global process is chosen as 4:1. We monitor the energy and the specific heat for each five Monte Carlo steps. In the case

TABLE I. Estimate of $E(\infty)$ based on the linear (second column) and quadratic (third column) approximations. The exact solution of Katsura (Ref. 14) is given in the fourth column.

	E_{linear}	$E_{\text{quadratic}}$	E_{exact}
$T = 0.1$	-0.634 75	-0.634 15	-0.633 98
$T = 0.2$	-0.625 75	-0.625 70	-0.625 70
$T = 0.3$	-0.610 44	-0.610 42	-0.610 49
$T = 0.4$	-0.587 70	-0.587 68	-0.587 68

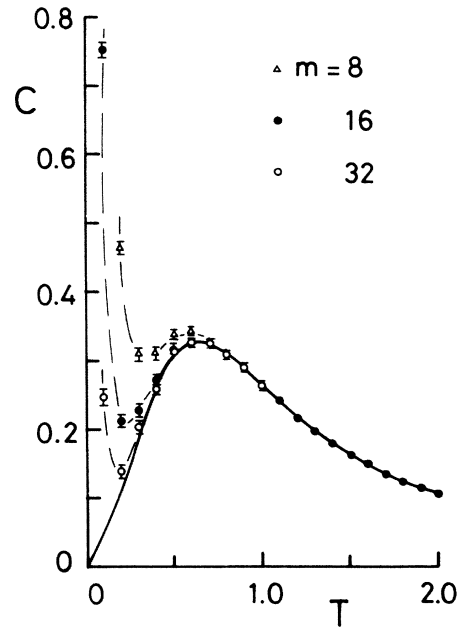


FIG. 7. Temperature dependence of specific heat for the one-dimensional XY model for $m = 8, 16$, and 32 . The solid curve is the exact solution of Katsura (Ref. 14).

of $N = 128$ and $m = 16$, it takes about 92 sec for the calculation of 4×10^5 Monte Carlo steps. It means that we update 17.8×10^6 classical spins per second. We have achieved the speed of the same order as the classical case.

We show the temperature dependence of energy per spin in Fig. 5. We measure the energy and temperature in units of J . The statistical errors are within 0.1%, and smaller than the mark. We have estimated the statistical

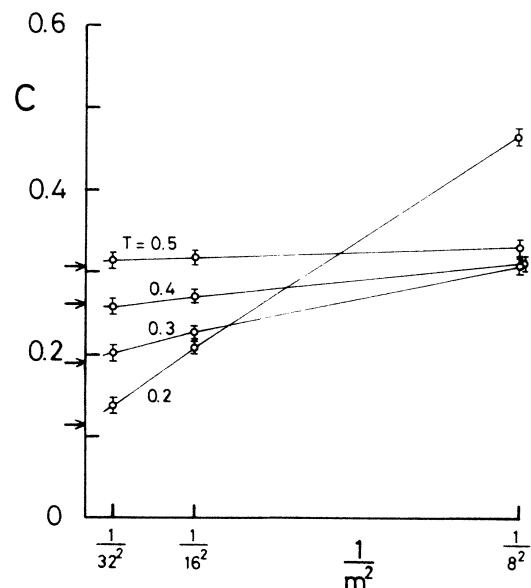


FIG. 8. Specific heat versus $1/m^2$ for the one-dimensional XY model at fixed temperatures. The arrows indicate the exact values obtained by Katsura (Ref. 14).

errors by the short-time calculations. The solid curve is the exact calculation of Katsura.¹⁴ We see that the calculated energy is very close to the exact one for large m even at extremely low temperatures. Suzuki¹⁵ has proved that the convergent rate of the average of the quantum operator is proportional to $1/m^2$. Betsuyaku² has plotted the energy versus $1/m^2$ for $m \leq 8$ to estimate the $m \rightarrow \infty$ value. We give the $1/m^2$ dependence of the energy for fixed T in Fig. 6. It is found that the energy quickly approaches the exact value. The estimate of the $m \rightarrow \infty$ value is given in Table I. In the second column we give the linear estimate,

$$E(m) = E(\infty) + a/m^2,$$

using the data for $m = 32, 16$. In the third column we give the quadratic estimate,

$$E(m) = E(\infty) + a/m^2 + b/m^4,$$

using the data for $m = 32, 16$, and 8 . The exact values are given in the fourth column. The agreement is surprisingly excellent.

The temperature dependence of specific heat per spin is shown in Fig. 7. We calculate the specific heat on the basis of Eq. (4). We have checked that the numerical differentiation of energy gives a consistent value. The statistical errors are within 2%. The error bars are given in the figure when the errors are larger than the mark. We see from the figure that the calculated specific heat is very close to the exact solution even at low temperatures. We show the $1/m^2$ dependence of the specific heat in Fig. 8. We see that the specific heat also approaches the exact value smoothly.

IV. SUMMARY AND DISCUSSIONS

In summary, we have implemented a high-speed algorithm for the Monte Carlo simulation of the quantum spin system. It should be emphasized that the idea of vectorization is a general one. The key point is to decompose the lattice into appropriate sublattices in each updating process. We have introduced the plaquette spin representation, which enables us to make a simple and fast calculation. This representation with the logical command XOR is restricted to the case of $S = \frac{1}{2}$ for the quantum spin system, but application to various fermion systems is possible. We have simulated the one-dimensional XY model using a high-speed algorithm. The agreement with

the exact solution is remarkable for large m . We have shown that the m th approximant of the energy and the specific heat approaches the exact values with the convergent rate of $1/m^2$ as was proved by Suzuki.¹⁵ There exist a lot of problems in various fields of which low-temperature behavior is uncertain because the Trotter number employed so far is small. It is hopeful that the high-speed technique we have presented will help advance many fields of quantum statistical Monte Carlo simulations.

ACKNOWLEDGMENTS

We wish to thank H. Betsuyaku and H. Nishimori for fruitful discussions. We also thank H. Katayama of NEC Corporation for valuable suggestions on computer programming.

APPENDIX

We present the expressions for $E_j^{(m)}$, $F_j^{(m)}$, and $G_j^{(m)}$. We use the plaquette spin representation for the local four-spin configuration:

$$E^{(m)}(0,4) = -(K_0 + \ln \cosh K_-) / \beta, \quad (\text{A1a})$$

$$E^{(m)}(1,5) = (K_0 - \ln \cosh K_+) / \beta, \quad (\text{A1b})$$

$$E^{(m)}(2,6) = (K_0 - \ln \sinh K_+) / \beta, \quad (\text{A1c})$$

$$E^{(m)}(3,7) = -(K_0 + \ln \sinh K_-) / \beta, \quad (\text{A1d})$$

$$F^{(m)}(0,4) = -(K_0 + K_- \tanh K_-) / \beta, \quad (\text{A2a})$$

$$F^{(m)}(1,5) = (K_0 - K_+ \tanh K_+) / \beta, \quad (\text{A2b})$$

$$F^{(m)}(2,6) = (K_0 - K_+ \coth K_+) / \beta, \quad (\text{A2c})$$

$$F^{(m)}(3,7) = -(K_0 + K_- \coth K_-) / \beta, \quad (\text{A2d})$$

$$G^{(m)}(0,4) = -[(K_- / \beta) \operatorname{sech} K_-]^2, \quad (\text{A3a})$$

$$G^{(m)}(1,5) = -[(K_+ / \beta) \operatorname{sech} K_+]^2, \quad (\text{A3b})$$

$$G^{(m)}(2,6) = [(K_+ / \beta) \operatorname{cosech} K_+]^2, \quad (\text{A3c})$$

$$G^{(m)}(3,7) = [(K_- / \beta) \operatorname{cosech} K_-]^2, \quad (\text{A3d})$$

where K_0 and K_{\pm} are defined by

$$K_0 = \beta J_z / (2m), \quad (\text{A4})$$

$$K_{\pm} = \beta (J_x \pm J_y) / (2m). \quad (\text{A5})$$

¹M. Suzuki, Prog. Theor. Phys. **56**, 1454 (1976); J. Stat. Phys. **43**, 886 (1986).

²H. Betsuyaku, Phys. Rev. Lett. **53**, 629 (1984); Prog. Theor. Phys. **73**, 319 (1985).

³T. Yokota and H. Betsuyaku, Prog. Theor. Phys. **75**, 46 (1986).

⁴H. Betsuyaku, Prog. Theor. Phys. **75**, 774 (1986); H. Betsuyaku and T. Yokota, *ibid.* **75**, 808 (1986).

⁵M. Suzuki, S. Miyashita, and A. Kuroda, Prog. Theor. Phys.

58, 1377 (1977).

⁶J. E. Hirsch, R. L. Sugar, D. J. Scalapino, and R. Blankenbecler, Phys. Rev. B **26**, 5033 (1982).

⁷J. L. Cullen and D. P. Landau, Phys. Rev. B **27**, 297 (1983).

⁸T. Sakaguchi, K. Kubo, and S. Takada, J. Phys. Soc. Jpn. **54**, 861 (1985).

⁹S. Wansleben, J. G. Zabolitsky, and C. Kalle, J. Stat. Phys. **37**, 271 (1984).

¹⁰C. Kalle, *J. Phys. A* **17**, L801 (1984).

¹¹M. Kikuchi and Y. Okabe, *Prog. Theor. Phys.* **74**, 458 (1985);
J. Phys. Soc. Jpn. **55**, 1359 (1986).

¹²M. Barma and B. S. Shastry, *Phys. Rev. B* **18**, 3351 (1978).

¹³A. Wiesler, *Phys. Lett.* **89A**, 359 (1982).

¹⁴S. Katsura, *Phys. Rev.* **127**, B1508 (1962).

¹⁵M. Suzuki, *Phys. Rev. B* **31**, 2957 (1985); *J. Math. Phys.* **26**,
601 (1985); *Phys. Lett.* **113A**, 289 (1985).